Pergamon

Geochimica et Cosmochimica Acta, Vol. 65, No. 9, pp. 1355–1366, 2001

0016-7037/01 $20.00 + .00

PII S0016-7037(00)00546-4

Molecular scale characteristics of Cu(II) bonding in goethite–humate complexes

TIM E. ALCACIO,[1] DEAN HESTERBERG,[1,*] JEFF W. CHOU,[2] JAMES D. MARTIN,[3] SUZANNE BEAUCHEMIN,[4] and DALE E. SAYERS[2]

[1]Department of Soil Science, Box 7619, North Carolina State University, Raleigh, North Carolina 27695-7619, USA
[2]Physics at North Carolina State University
[3]Chemistry at North Carolina State University
[4]Agriculture and Agri-Food Canada, St. Foy, Quebec, Canada

(*Received March* 22, 2000; *accepted in revised form December* 5, 2000)

Abstract—Interactions between oxide minerals and natural organic matter affect metal adsorption properties of mineral surfaces, but the mechanisms of metal bonding are not well understood. Extended X-ray absorption fine structure (EXAFS) spectroscopy analyses were performed on aqueous pastes containing Cu(II) and goethite (α-FeOOH) with humic acid adsorbed at 0, 14, 28, 57, 88, 216, and 236 g kg^{-1} goethite, and with aqueous suspensions of humic acid only. Analyses were conducted at the Cu K edge with 40 mmol Cu(II) kg^{-1} goethite or 2 mmol Cu(II) kg^{-1} suspension for the humic acid system. Samples were equilibrated at pH 5.6 in a 0.1 M $NaNO_3$ background electrolyte. For all systems, analysis of EXAFS results suggests that Cu(II) is present in a distorted octahedral configuration containing four short equatorial (1.94–1.97 Å) and two longer axial bonds with oxygen. When the concentration of adsorbed humic acid on goethite was increased from 0 to 28 g kg^{-1}, the axial Cu-O bond length decreased to 2.24 ± 0.03 Å, which was less than for individual humic acid (2.32 ± 0.02 Å) or goethite (2.29 ± 0.03 Å) samples. The apparent decrease in the axial Cu-O bond length was attributed to a decrease in the ligand field splitting energy. When humic acid ligands replace equatorial water molecules in the Cu(II) coordination sphere, a weaker ligand field strength occurs. For absorbed humic acid up to 88 g kg^{-1} goethite, second-shell iron neighbors were observed between 3.17 and 3.20 Å, suggesting that Cu(II) was bonded on average to both inorganic (goethite) and organic (humic acid) functional groups. In addition, derivative X-ray absorption near edge structure (XANES) spectra for Cu(II) on goethite–humate complexes (<88 g kg^{-1}) were poorly fit by use of a linear combination of spectra for Cu(II) on goethite or humate alone. At humate concentrations between 216 and 236 g kg^{-1} goethite, second-shell iron neighbors could not be identified, and the Cu-O_{axial} distance (2.32 ± 0.02 Å) and derivative XANES spectra strongly resembled that of Cu(II) adsorbed to humate only. Analysis of the XANES and EXAFS data suggested that Cu(II) was bonded on average to both inorganic and organic functional groups as a type A ternary complex at lower levels of adsorbed humate, and to organic groups as a type B complex at higher levels.

1. INTRODUCTION

In soils, phyllosilicate and oxide minerals are often found associated with organic matter (Oades, 1988). Organic matter on mineral surfaces at concentrations as low as 10 g kg^{-1} may influence the mobility and bioavailability of contaminants adsorbed in soil (Bertsch and Seaman, 1999). Associations involving humic acid, a chemically reactive fraction of natural organic matter, have been found to affect the adsorption of organic and inorganic contaminants to mineral surfaces (Davis, 1984; Schellenberg et al., 1994).

Iron, aluminum, and manganese oxide minerals are particularly important in soils because of their high (pH dependent) affinity for heavy metal cations and oxyanions, which often bond through inner-sphere surface complexes (Bertsch and Seaman, 1999). Certain metal cations such as Cu(II), Hg(II), and Pb(II) also have a greater bonding affinity for humic acid than other cations (Kerndorff and Schnitzer, 1980). The heterogeneous nature of humic acids causes the metal binding properties to be very complicated. For example, Cu(II) bonds more strongly to natural organic matter at low levels of Cu(II) (Buffle, 1988). This phenomenon has been attributed to selective binding at high-affinity sites such as amine, polyphenol, and sulfhydryl groups (Stevenson, 1994). The molecular configuration of metal bonding to humic acid is difficult to assess experimentally. Humic acid also binds strongly to iron oxide mineral surfaces by inner-sphere surface complexation (McBride, 1994). Thus, in a system consisting of organic matter associated with a mineral surface, possible binding arrangements include metal cations bonded to the mineral surface only, metal cations bonded to adsorbed organic matter that is itself bound to the surface (type B ternary complex), or a bonding arrangement that involves cation bridging between clay and organic bonding sites (type A ternary complex; Fig. 1; McBride, 1994).

It is possible that the solubility of Cu(II) observed in macroscopic experiments may stem from the reactivity of specific metal binding sites. For example, Tipping et al. (1983) found that Cu(II) sorption increased when humic acid was adsorbed to goethite. The binding was attributed to higher energy sites created by the interaction between goethite and humic acid, rather than from additional sites contributed by the humic acid. At the molecular level, the structure of such binding sites may involve ligands containing inorganic and organic functional groups that form type A ternary complexes. In contrast, Davis (1984) found that the sorption of Cu(II) to γ-Al_2O_3 in the presence of adsorbed organic matter was similar to that for

*Author to whom correspondence should be addressed (dean_hesterberg@ncsu.edu).

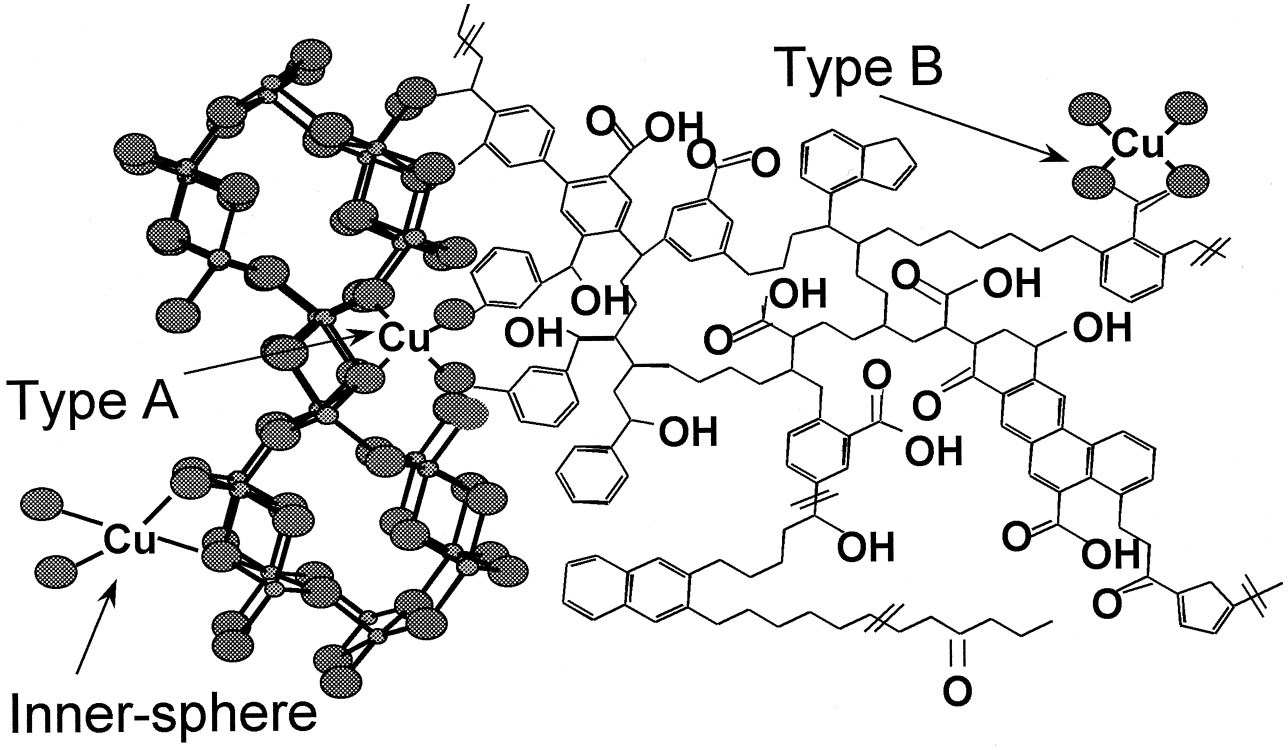

Fig. 1. Illustration of some possible bonding configurations of Cu(II) on goethite–humate complexes: inner-sphere complexation of Cu(II) at goethite sites, and type A and B ternary complexes.

dissolved Cu(II)–organic complexes. This result suggested that on the molecular level, type B complexes may have formed, where the cations bond to the adsorbed organic matter. Robertson and Leckie (1994) found that pH-dependent Cu(II) binding in mixtures of goethite and humic acid was not a simple linear combination of binding properties of the single component systems, but Cu(II) binding by humic acid was diminished by the presence of goethite. The authors offered the possibility that goethite competes with Cu(II) for humic acid binding sites.

The aim of the present research was to better understand on a molecular level the nature of metal bonding in a clay–organic complex, specifically Cu(II) on goethite (α-FeOOH) with adsorbed humic acid. Molecular-scale research has addressed binding of organic matter to mineral surfaces and metal bonding to clay and oxide minerals or organic matter, but few have performed a structural analysis of metal bonding in clay–organic systems. EXAFS studies of Cu(II) bonding at goethite surfaces (Bochatay et al., 1997; Parkman et al., 1999) and by humic acids (Xia et al., 1997; Korshin et al., 1998) showed that Cu(II) forms a distorted octahedron with the extent of distortion differing between the two sorbents. One study involving Cu(II) bonding with illite–humate complexes suggested that Cu-O distances were less than those in the absence of adsorbed humic acid (Hesterberg et al., 1997).

The objective of this study was to determine whether Cu(II) bonding with goethite–humate complexes primarily involves coordination with inorganic or organic binding sites, or with unique sites that involve both inorganic and organic functional groups.

2. EXPERIMENTAL METHODS

2.1. Synthesis and Characterization of Goethite

Goethite (α-FeOOH) was synthesized by oxidizing dissolved $FeCl_2 \cdot 4H_2O$ for 48 h (Schwertmann and Cornell, 1991). Poorly crystalline iron oxide phases were removed by reacting the goethite with a mixture of 0.2 M $NH_4C_2O_4$ + 0.2 M HC_2O_4 in the dark for 2 h (Kunze and Dixon, 1986). The goethite was washed once with 1 M NaCl to remove dissolved oxalate and washed multiple times with deionized water to reduce the ionic strength. The mineral was concentrated into a paste and reacted with 30% H_2O_2 and heated to 85°C for 10 min to remove surface-bound organic residues. After washing with deoxygenated and deionized water, the dispersed goethite was gravity settled and the <2-μm fraction collected (Gee and Bauder, 1986). The stock suspension of the <2-μm fraction containing 36.3 g goethite kg^{-1} in deionized water was stored at 3°C. A representative subsample of the stock suspension was freeze dried and analyzed by X-ray diffraction (Co Kα radiation) to confirm the mineralogical purity. The final goethite sample surface area, measured by the single-point BET method (Quantachrome Monosorb), was 93 ± 3 m^2 g^{-1}. Organic carbon (5.5 g C kg^{-1}) on the dried samples was measured by the Walkley Black method (Nelson and Sommers, 1996).

2.2. Soil Collection and Humic Acid Extraction

Soil samples were collected from a created *Spartina alterniflora* salt marsh located on the west bank of the Newport River Estuary (34°45′N, 76°40′W) near Morehead City, North Carolina, USA (Broome and Craft, 2000). The wet samples were double sealed into low-density polyethylene bags and immediately placed in ice. Plant roots and other debris were removed by passing the sample sequentially through 5-mm and 2-mm stainless steel sieves. To preserve the state of reduced organic sulfur in the soil organic matter, this step and all sample preparation work were performed in a glove box under an oxygen-scrubbed Ar(g) atmosphere and under a safe light. The <2-mm

fraction was homogenized with a rotary mixer with a stainless steel propeller blade, and the water content was determined gravimetrically by oven-drying the subsamples at 110°C. The sample was divided into 250 g (oven dry weight basis) subsamples that were sealed individually in low-density polyethylene bags and stored in a freezer until the humic acid was extracted.

The humic acid extraction procedure followed the protocol of the International Humic Substance Society (Swift, 1996), with some notable modifications. To prevent sample exposure to oxygen and ultraviolet light, all steps except filtering and HCl-HF washing were performed under an Ar(g) atmosphere and a safe light. All reagents were prepared daily in oxygen-free water, which was prepared by boiling the deionized water, purging with oxygen-scrubbed N_2(g) while cooling, and storing in glass containers.

Twelve 20-g subsamples of <2-mm soil were placed into 250-mL polypropylene centrifuge bottles and acidified with HCl to pH 2 (Swift, 1996). Composites of six subsamples were placed into two 2-L high-density polyethylene bottles, and the samples were adjusted to pH 12 with NaOH. After bringing the final volume to 1.2 L with deionized water, the samples were shaken for 4 h according to the International Humic Substance Society procedure. The samples were divided again into the 12 centrifuge bottles and centrifuged at 1500 × *g* for 10 min. The supernatant solutions were decanted into two 2-L bottles. The solutions were acidified to pH 1 and set aside for 16 h to flocculate the humic acid (Swift, 1996). The acidified suspensions were centrifuged, and the supernatant solutions containing fulvic acid were decanted.

The settled humic acid was resuspended with 0.1 M KOH, rinsed into a single 1-L bottle, and brought to pH 11 and 550 mL volume by adding 1 M KOH and deionized water. Solid KCl was added to obtain a 0.3 M KCl background solution (Swift, 1996), and the sample was shaken for 30 min and centrifuged for 4 h at 45,000 × *g* to reduce the ash content (inorganic components). To further reduce the ash content, the supernatant solution was passed through syringe filters with 0.2-μm pores (Gelman Supor). After adjusting to pH 1 with HCl, the humic acid was concentrated by centrifugation, then washed two times with 0.1 M HCl and 0.3 M HF to remove inorganic residues (Swift, 1996). To exchange Cl^- with NO_3^- (the background anion used in subsequent experiments), the humic acid was resuspended at pH 2.3 by adding deionized water and NaOH, and $NaNO_3$ salt was added to yield a 0.3 M $NaNO_3$ background solution. The sample was brought to pH 2 with HNO_3, shaken for 30 min and centrifuged at 9000 × *g*; next, the clear supernatant solution was decanted. The humic acid was then repeatedly washed with deionized water and centrifuged until the supernatant solution tested negative for Cl^- ($AgNO_3$ test).

The humic acid was freeze dried, and total carbon (480 ± 3 g kg^{-1}) and nitrogen (48.0 ± 0.4 g kg^{-1}) were measured by combustion with a CHN analyzer (Perkin Elmer). A portion was digested by use of 30% H_2O_2 to oxidize organic sulfur, and sulfate was measured (18 ± 1 g S kg^{-1}) by ion chromatography (Dionex) with an AS-4A column (Douek and Ing, 1989).

2.3. Humate Sorption to Goethite

Samples containing humate and goethite were prepared in a 0.1 M $NaNO_3$ background solution at pH 5.6, and they were prepared with different levels of adsorbed humic acid. All samples were prepared in deoxygenated water as before. While working under an Ar(g) atmosphere and a safe light, 12.4 g of well-mixed goethite stock suspension (containing 0.45 g goethite on a dry weight basis) were added to each of five 40-mL Teflon centrifuge tubes. The samples were centrifuged at 9000 × *g* for 20 min to remove excess water. The amount of entrained water was determined gravimetrically to ensure that it did not dilute the final samples more than 3%.

In a separate 50-mL sample bottle, the freeze-dried humic acid was dissolved in 0.1 M $NaNO_3$ adjusted to pH 11 with 0.1 M NaOH. The sample was shaken vigorously for 1 h, and the pH was checked periodically. Before adding the humate suspension, the goethite in each centrifuge tube was resuspended in 0.1 M $NaNO_3$, and 0.1 M NaOH was added to bring the pH to 8 while each mineral suspension was stirred continuously, an appropriate amount of humate stock was slowly added corresponding to 0, 15, 30, 60, 90, 220, or 240 g kg^{-1} goethite. The goethite–humic acid suspensions were acidified to pH 5.6 with 0.1 M HNO_3; then the suspension mass was brought to 35 g.

The samples were shaken for 18 h at 25°C in a reciprocating water-bath shaker; then the pH was checked and adjusted to pH 5.6 as needed with 0.1 M HNO_3. Shaking was continued for a total of 24 h before centrifuging (9000 × *g* for 20 min). The suspension mass was increased to 36 g (12.5 g goethite kg^{-1}) with 0.1 M $NaNO_3$; the final Na concentration was 0.1 M. The supernatant solution was analyzed for dissolved organic carbon by high-temperature catalytic combustion on a Shimadzu 5050 TOC analyzer.

Weakly adsorbed organic matter and dissolved organic carbon were removed from the goethite suspensions by washing five times with 0.1 M $NaNO_3$. The washing procedure involved bringing the mass of the suspension to 36 g and shaking for 20 min. The supernatant solutions were analyzed for dissolved organic carbon. Assuming a constant level of 480 g organic carbon kg^{-1} humic acid, it was found that the actual amounts of sorbed humic acid were 0, 14, 28, 57, 88, 216, and 236 g kg^{-1} goethite.

On the basis of these sample preparation methods, essentially all humic acid in the goethite–humic acid samples should be adsorbed, not precipitated. A separate experiment to determine humic acid adsorption characteristics on goethite yielded an adsorption isotherm (data not shown) characterized as an L-curve (Sposito, 1984), with a maximum level of 280 g adsorbed humic acid kg^{-1} goethite at pH 5.6 in 0.1 M $NaNO_3$ background solution. Furthermore, for samples of humic acid alone at pH 5.6 in a 0.1 M $NaNO_3$ background solution and various levels of adsorbed Cu(II), we could not separate humic acid by extensive centrifugation. Also, in preparing the humic acid, a pH of <3 (in 0.3 M $NaNO_3$ background solution) was required to precipitate and separate the material by centrifugation.

2.4. Copper(II) Sorption to Humate/Goethite Samples

After humic acid was adsorbed, the entrained solution in each sedimented sample was determined, and the mass of the suspension was brought to 34 g with 0.1 M $NaNO_3$. The suspensions were adjusted to pH 5 with 0.1 M HNO_3. Under an Ar atmosphere, 517 μL of 35 mM $Cu(NO_3)_2$ (pH 3) was added slowly to each centrifuge tube while the contents were stirred vigorously. Thermodynamic equilibrium calculations of the resulting solution were performed using MINTEQA2 (Allison et al., 1990), with constants supplied by Lindsay (1979). The calculations indicated that at the initial Cu(II) concentration added (assuming no adsorption), the solution was undersaturated with respect to $Cu(OH)_2$ and CuO, with 99% of Cu(II) present as Cu^{2+} (aq). The suspensions were adjusted to pH 5.6 with 0.1 M NaOH and capped. The final mass of each suspension was 36 g, and the Na concentration was 0.1 M. The centrifuge tubes were wrapped in aluminum foil and shaken for 24 h. During the 24-h period, the pH was periodically checked. The suspensions were centrifuged (9000 × *g* for 20 min) and decanted, and the dissolved Cu concentrations were determined by use of atomic absorption spectrometry (Perkin Elmer). For all samples, at least 98% of the initially added Cu was adsorbed, so the final concentrations were 40 mmol Cu(II) kg^{-1} goethite. The Cu–humate/goethite pastes were then sealed under Ar (g) and stored at 3°C for EXAFS analysis.

To produce a sample of Cu(II) bound to humic acid only, an aliquot of stock solution containing 20 mg of humic acid was added to a 40-mL Teflon centrifuge tube. The mass of the suspension was increased to 8 g with 0.1 mol/L $NaNO_3$, and the pH was decreased to pH 5 with 0.1 M HNO_3. A 575-μL aliquot of 35 mM $Cu(NO_3)_2$ solution was added to yield a Cu concentration of 2 mmol kg^{-1} suspension. The suspension was adjusted to pH 5.6 with 0.1 M NaOH. The sample mass was increased to 10 g with 0.1 M $NaNO_3$, and the samples were shaken at 25°C for 24 h. The final pH was 5.6 ± 0.1.

2.5. EXAFS Data Collection

EXAFS data for goethite and humic acid samples were collected at the National Synchrotron Light Source, Brookhaven National Laboratory, Upton, NY, at beamline X-11A. The electron storage ring operated at 2.528 GeV, with maximum beam current at 300 mA. The monochromator consisted of two parallel Si(111) crystals. Samples were mounted in a Plexiglas holder and aligned 45° to the incident beam. As a reference for the edge position, the spectrum of a metallic Cu foil was collected in transmission mode behind the sample. The

reference K edge (E_0 = 8987 eV) was assigned to the maximum of the first derivative of the Cu foil spectrum. Fluorescence spectra for goethite and humate samples were collected with a 13-element Ge solid-state detector. Six to 10 scans were collected at room temperature and averaged to improve the signal to noise ratio. Energy shifts caused by the drifting of the monochromator were corrected by referencing to the apparent edge position of the Cu metal foil. The vertical position of the 0.5-mm premonochromator slit was optimized periodically to correct for any movement in beam position.

2.6. EXAFS Data Analysis

Standard methods were employed for analyzing the extended X-ray absorption fine structure (EXAFS) spectroscopy data (Sayers and Bunker, 1988). By use of the computer program MacXAFS 4.1 (Bouldin et al., 1995), the background was subtracted from the raw adsorption data by use of a modified cubic spline technique that consisted of three knots at unequal distances. The data were cube weighted (w = 3) to compensate for damping of the EXAFS spectrum at higher energies. The data were converted to a wave vector and Fourier transformed (k = 2.56–10.91 Å^{-1}) to isolate first- and second-shell components. Single point glitches caused by the monochromator were deleted from the data. In some instances, the glitch spanned several inverse angstroms (7.0–7.5 Å^{-1}) and could not be removed. The Fourier-transformed spectra were fit in R-space using FEFFIT. The R-space fitting range for goethite and goethite–humate samples was 1.00 to 3.23 Å, and the fitting range of the humate only sample was 1.00 to 2.76 Å. The number of fitting parameters did not exceed the number of independent points (N_{IDP}) throughout the fitting process, where $N_{IDP} = (2\ \Delta k\ \Delta R/\pi)$, where Δk is the k range being fit and ΔR is the width of the R-space Fourier window (Lytle et al., 1988).

The Debye-Waller factor (σ^2), which accounts for thermal and static disorder, was fixed at 0.008 for intermetallic (Cu-Fe) fitting and 0.006 for distorted first-shell (Cu-O_{axial}) neighbors. These fixed values corresponded closely to those found in the literature (Bochatay et al., 1997; Xia et al., 1997; Korshin et al., 1998; Fitts et al., 1999; Parkman et al., 1999). In addition, the Debye-Waller factors are within the range that we determined when fitting known organic and inorganic Cu(II) standards. Phase shifts from oxygen backscattering were obtained experimentally by a FEFF 6.0 (Zabinski et al., 1994) generated file of tenorite (CuO). Tenorite possesses a 4 + 2 distorted octahedral arrangement that contains two O at 1.95 Å, two O at 1.96 Å, and two O at 2.78 Å (Asbrink and Norrby, 1970). For the fitting of Cu-Fe coordination shells, an input file was created in which Cu was substituted for Fe atoms in goethite located at 2.90 Å. An S_0^2 value of 0.75 was obtained from the analysis of equatorial Cu-O coordination numbers determined by FEFF 6.0 for an actual tenorite standard (Aldrich Chemicals). Because of the high signal to noise ratio (40) in our study and the accuracy of modern ab initio EXAFS codes, all final EXAFS best-fit indexes (R^2) were <2%. The R^2 index is similar, though not identical, to the reduced χ^2, where lower values equate with higher confidence limits (Lytle et al., 1988). Standard errors reported for fitting parameters were those calculated by MacXAFS 4.1 (Bouldin et al., 1995).

2.7. XANES Analysis

Copper K X-ray absorption near edge structure (XANES) spectra were quantitatively analyzed by use of a combination of principal component analysis (PCA) and linear combination fitting. To define the number of independent absorbing components in the XANES spectra for the samples containing Cu(II) bound to goethite–humate complexes, PCA was performed on the data matrix composed of six normalized K-XANES spectra and first-derivative XANES spectra for these samples (Malinowski, 1991). The normalized spectra (background and baseline corrected) and first-derivative spectra were interpolated to fit the same energy scale. By use of target transformation, two criteria, the SPOIL value and the F-test, were used to determine whether the spectra of the end-member standards (Cu(II) on goethite and Cu(II) on humic acid) could adequately represent spectral features of the six samples containing goethite with adsorbed humic acid. According to Malinowski (1991), tested targets (in this, case Cu(II) on goethite and Cu(II) on humic acid) with SPOIL values between 3 and 6 represent marginal targets. In the one-tailed F-test proposed by Malinowski (1991), the null hypothesis tests whether the target (standard spectrum) is an acceptable solution. Thus, the tested target is retained as valid when the probability of the calculated F is greater than a given critical threshold value such as 0.05 (5% probability). Furthermore, linear combination fitting (Vairavamurthy et al., 1997) was used to fit derivative XANES spectra for the samples containing the goethite–humate complex, using Cu(II) on goethite or humic acid as end-member standards. This nonlinear, least-squares fitting procedure computed the fractions of end-member (standard) spectra that (when summed) yielded the best fit (lowest χ^2) to the spectrum for a Cu–goethite–humate sample.

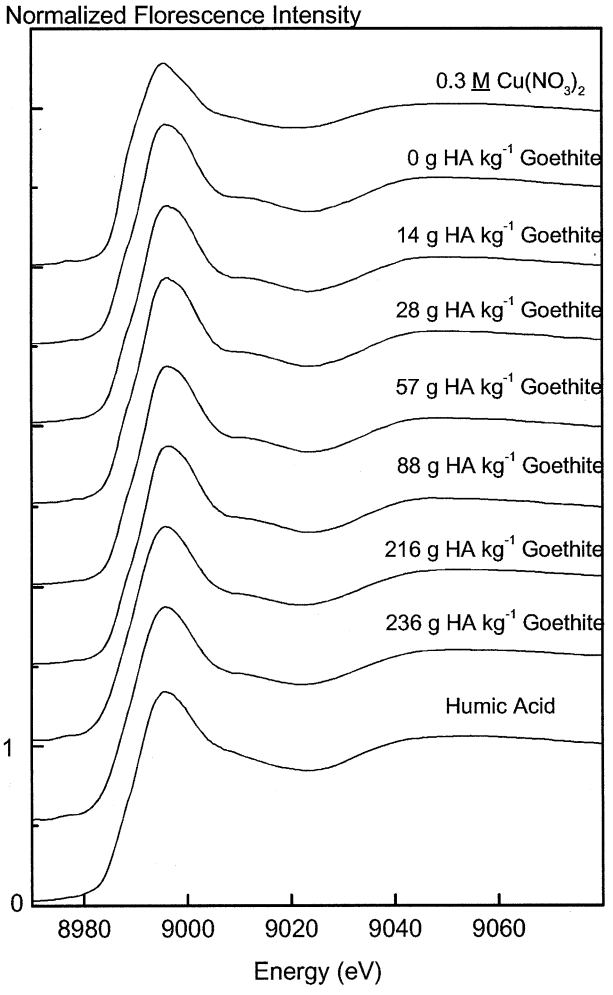

Fig. 2. Stacked, normalized X-ray Cu K-XANES spectra of aqueous $Cu(NO_3)_2$ solution, Cu(II) on goethite with varying levels of adsorbed humic acid, and Cu(II) on humic acid.

3. RESULTS

3.1. Cu-K XANES Spectra

Figure 2 shows the normalized XANES spectra for Cu(II) in aqueous solution, adsorbed on humic acid or goethite, and adsorbed on goethite–humate complexes. The XANES spectra appear to be very similar, with white-line peaks at 8995 eV. First derivative spectra (Fig. 3) for adsorbed Cu(II) show that the absorption edges in Figure 2 have two different inflections corresponding to derivative peaks at 8986 eV (α peak) and 8991 eV (β peak). The β peak represents the main absorption

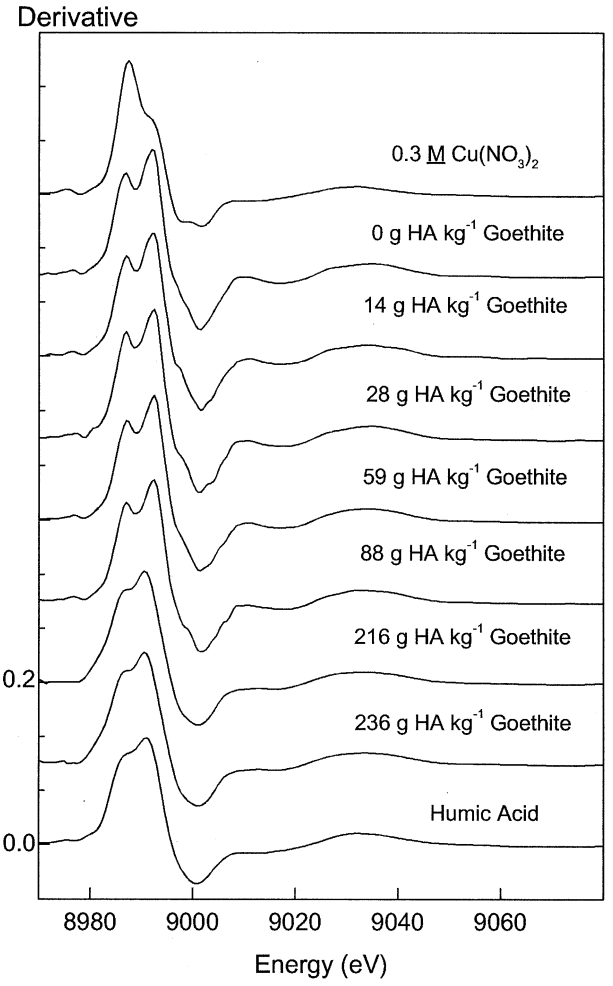

Fig. 3. Stacked, first-derivative Cu K-XANES spectra for the data shown in Figure 2.

transition (1s → continuum). The α peak, on the low energy side of the β peak in Figure 3, is influenced by the degree of bond covalency and the degree of local structural disorder (Kau et al., 1987; Palladino et al., 1992). The α peak intensity for the aqueous 0.3 M $Cu(NO_3)_2$ solution was greater than for all of the adsorbed Cu(II) samples. With increasing amounts of adsorbed humic acid (0–88 g kg^{-1}), the α peak in the normalized derivative spectra became less intense. At adsorbed humate concentrations $\geq$ 216 g kg^{-1}, the α intensity approached a minimum value and the spectra more strongly resembled Cu(II) adsorbed to humic acid only. This result suggested that Cu(II) was principally bonded to the adsorbed humic acid rather than goethite and formed type B ternary complexes (goethite–humate-Cu) at higher surface loading of humate.

PCA performed on the normalized K-XANES spectra of the six Cu samples containing goethite with adsorbed humic acid revealed two significant components. However, neither XANES spectra for Cu(II) on goethite nor Cu(II) on humic acid came out as likely targeted species for describing the sample spectra because SPOIL values equaled 9.9 and 7.8, respectively, and probabilities of F values for both standards were 0.0001 (i.e., $<$0.05). This result indicated that some other

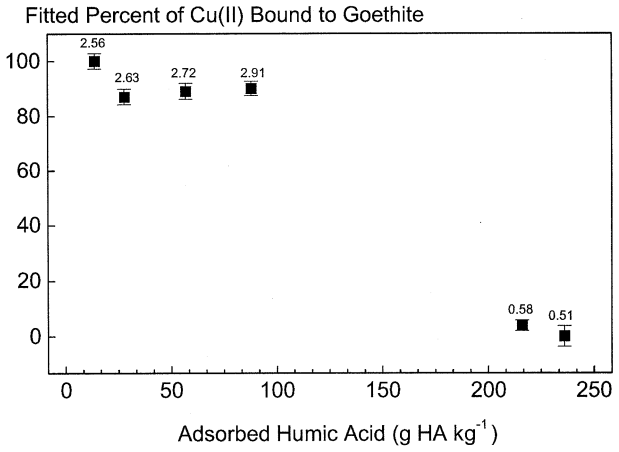

Fig. 4. Results of linear combination fitting analysis with Cu–goethite and Cu–humic acid bonding as fitting standards. Data show the percentage of Cu–goethite spectrum giving the best fit. χ^2 values are noted above each data point.

chemical species would better fit the spectra of samples containing the goethite–humate complex. In the case of the first derivative spectra, which show distinct α and β peaks, PCA indicated that three significant components were needed to describe the sample data. The standard of Cu(II) on goethite was an acceptable species (SPOIL = 1.75; probability $F >$ 0.05), whereas Cu(II) on humic acid was a marginal species (SPOIL = 5.07; probability $F <$ 0.05). This result suggests that the samples with Cu(II) on goethite–humate complexes contain at least one additional chemical species with derivative XANES spectral features that are unique compared with those of Cu(II) on either goethite or humic acid.

Figure 4 shows results of linear combination fitting of the derivative XANES spectra for Cu(II) in goethite–humate samples by use of Cu(II) on goethite only and Cu(II) on humic acid as fitting standards. These results showed no particular trend with increasing humic acid loading on goethite. If Cu(II) was partitioning between inorganic and organic functional groups in proportion to adsorbed humic acid level, then one would expect a linear decrease in Cu(II) goethite character with increasing adsorbed humic acid level. However, Figure 4 shows that Cu(II) in the goethite–humic acid systems retained characteristics of Cu(II) on goethite for adsorbed humic acid up to 88 g kg^{-1}. At adsorbed humic acid levels $\geq$ 216 g kg^{-1}, derivative XANES spectra were best fit as nearly 100% Cu(II) bonded to humic acid, which supports the notion that Cu(II) was bound to the adsorbed humic acid (type B ternary complex). The goodness of fit (χ^2 values) for the linear combination fitting results shown in Figure 4 were 2.56, 2.63, 2.72, 2.91, 0.58, and 0.51 for humic acid loadings of 14, 28, 57, 88, 216, and 236 g kg^{-1} goethite, indicating that the combination of the end-member standards gave a poorer fit for the samples with loadings between 14 and 88 g kg^{-1} compared with those at loadings of 216 and 236 g kg^{-1}.

On the basis of the following observations, XANES and derivative XANES spectral analyses support the hypothesis that type A ternary complexes were significant in the four goethite–humate samples containing adsorbed humic acid $\leq$ 88 g kg^{-1}: (1) PCA analysis indicated that the spectra have

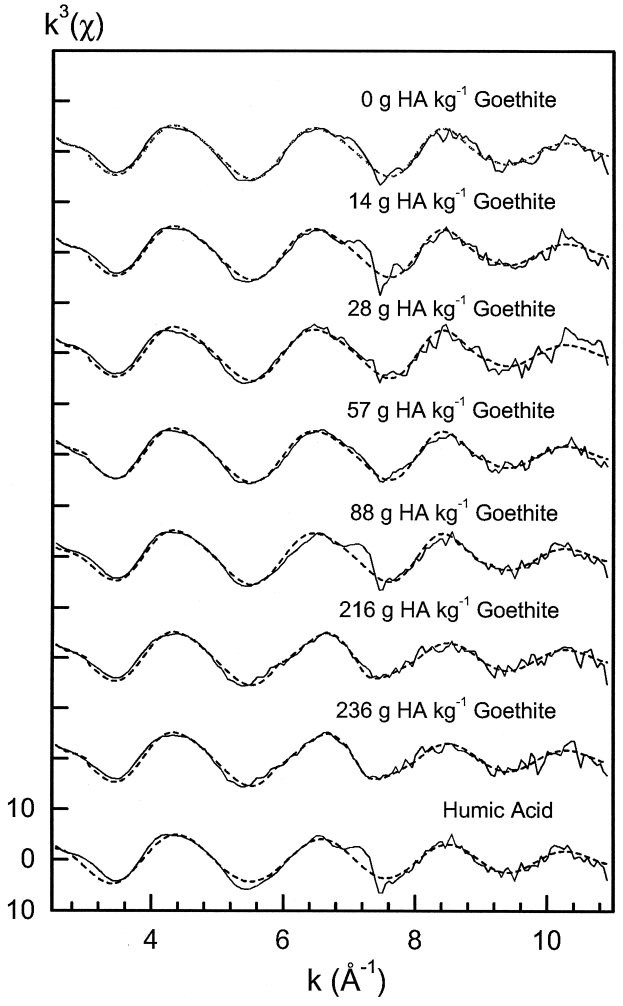

Fig. 5. Stacked, normalized k^3-weighted EXAFS spectra for Cu(II) in aqueous solution, on goethite, on goethite with adsorbed humic acid, and on humic acid only. Solid and dotted lines represent the normalized data and best fits, respectively.

characteristics that are not fully accounted by the spectra for Cu(II) on either goethite or humic acid alone; (2) linear combination fitting indicated that derivative XANES spectra for these samples are better characterized by Cu(II) on goethite than Cu(II) on humic acid, with no linear trend with increasing humic acid; and (3) poorer fits (greater χ^2) were obtained for these four samples compared with the two samples with higher levels of adsorbed humic acid where analysis of XANES data indicated the dominance of a type B ternary complex.

3.2. Cu-K EXAFS Spectra

Normalized k^3-weighted EXAFS spectra for aqueous Cu(II) and the various adsorbed species are presented in Figure 5, along with the modeled EXAFS spectra generated from the fitting results in Table 1. The weighting factor produces an EXAFS spectrum with oscillations of about equal amplitude across the entire k range, but it also amplifies spectral noise at high k (Sayers and Bunker, 1988). Some of the data in Figure 5 also contained a glitch from 7 to 7.5 $Å^{-1}$ that consisted of several data points in some cases and could not be removed. Figure 6 shows the radial structure functions (RSFs) derived from Fourier transformations of the k^3-weighted EXAFS spectra in Figure 5.

The position of the peaks in the RSFs correspond to relative distances (uncorrected for phase shift) between Cu(II) and atoms in local coordination shells. The strongest peak, occurring between 1.56 and 1.59 Å in Figure 6, corresponds to first-shell O atoms. A weaker peak representing additional first-shell O atoms was also distinguishable above the background spectral noise between 2.1 and 2.3 Å. The spectra for most samples containing goethite displayed a distinct single peak between 2.7 and 3.0 Å, which is due to iron neighbors (Fig. 7, discussed below). This peak is not present for goethite samples with adsorbed humic acid levels $\geq$ 216 g kg^{-1}. The presence of iron in the second coordination shell indicates that Cu(II) was bonded (on average) as an inner-sphere complex on the goethite surface. Also, from Figure 6, differences in the imaginary part of the Fourier transform between Cu(II) on goethite vs. Cu(II) on goethite with absorbed humic acid can be seen. Furthermore, the imaginary parts for Cu(II) on goethite with humic acid adsorbed at 216 and 236 g kg^{-1} are essentially identical to that for Cu(II) on humic acid.

Quantitative EXAFS fitting results are shown in Table 1, and the goodness of fit can be seen from the modeled Fourier-transform magnitude and imaginary parts in Figure 6. For all samples, the average coordination environment of Cu(II) was reflective of distorted octahedra. The strong first-shell peak with a maximum between 1.56 and 1.59 Å (Fig. 6) corresponds to first-shell equatorial Cu-O bonds ($Cu\text{-}O_{eq}$) at (phase-shift corrected) distances of 1.94 to 1.97 Å (Table 1). The weaker peak, with a maximum between 2.1 and 2.3 Å (Fig. 6), contains contributions from both axial and equatorial Cu-O bonds. Axial Cu-O bonds ($Cu\text{-}O_{axial}$) have (corrected) distances between 2.24 and 2.32 Å (Table 1).

For samples containing humic acid, nitrogen and carbon cannot be easily distinguished from oxygen in the fitting of the EXAFS spectra. However, Cu-N bonding was discounted and excluded from the fitting for the following reasons. Previous EXAFS investigations of Cu(II) bonding with humic acid have identified $Cu\text{-}O_{axial}$ bonds with coordination distances that are slightly less (2.02–2.13 Å) than we found (Xia et al., 1997; Korshin et al., 1998). Frenkel and Korshin (1999) performed ab initio calculations of the XANES region for Cu(II) on humic acid and suggested that Cu-N bonding best explained the data. However, analysis of our XANES data indicated that they did not exhibit the necessary near edge features that suggest Cu-N bonding. In other studies that have investigated Cu(II) interactions with humic acid by use of electron paramagnetic resonance spectroscopy, the ligand environment was dominated by oxygen atoms (McBride, 1978; Bloom and McBride, 1979; Boyd et al., 1981a). One study did suggest minor amounts of Cu-N bonding in dried fulvic acids extracted from sewage sludge; however, aqueous suspensions were dominated by Cu-O bonding (Senesi and Sposito, 1984). We also excluded the possibility that the neighbors at 2.24 to 2.32 Å were due to second-shell carbon atoms. In copper(II) acetate, carboxylic acid functional groups are bonded to Cu(II) atoms, with second (Cu-O-C) crystallographic angles and distances of ~125° and

Table 1. EXAFS spectra fitting results.

Humic acid loading	Neighboring atom	Distance (Å)	Coordination no.	Debye-Waller ($Å^2$)	ΔE
0 g/kg	$Cu\text{-}O_{eq}$	1.96 ± 0.01	5.51 ± 0.90	0.007 ± 0.001	−11.22
	$Cu\text{-}O_{ax}$	2.29 ± 0.03	1.58 ± 0.70	0.006[a]	
	Cu-Fe	3.20 ± 0.05	0.58 ± 0.39	0.008[a]	
14 g/kg	$Cu\text{-}O_{eq}$	1.96 ± 0.01	5.00 ± 0.66	0.003 ± 0.001	−8.59
	$Cu\text{-}O_{ax}$	2.27 ± 0.02	1.49 ± 0.57	0.006[a]	
	Cu-Fe	3.18 ± 0.02	0.97 ± 0.31	0.008[a]	
28 g/kg	$Cu\text{-}O_{eq}$	1.96 ± 0.01	4.56 ± 0.63	0.007 ± 0.001	−10.29
	$Cu\text{-}O_{ax}$	2.24 ± 0.03	1.09 ± 0.60	0.006[a]	
	Cu-Fe	3.18 ± 0.02	0.70 ± 0.29	0.008[a]	
59 g/kg	$Cu\text{-}O_{eq}$	1.97 ± 0.01	5.16 ± 0.83	0.006 ± 0.001	−11.30
	$Cu\text{-}O_{ax}$	2.29 ± 0.02	1.30 ± 0.63	0.006[a]	
	Cu-Fe	3.17 ± 0.05	0.43 ± 0.35	0.008[a]	
88 g/kg	$Cu\text{-}O_{eq}$	1.97 ± 0.01	6.32 ± 0.97	0.010 ± 0.001	−12.60
	$Cu\text{-}O_{ax}$	2.30 ± 0.01	2.27 ± 0.65	0.006[a]	
	Cu-Fe	3.20 ± 0.03	0.79 ± 0.38	0.008[a]	
216 g/kg	$Cu\text{-}O_{eq}$	1.94 ± 0.01	5.17 ± 0.76	0.006 ± 0.001	−10.36
	$Cu\text{-}O_{ax}$	2.31 ± 0.02	1.12 ± 0.57	0.006[a]	
236 g/kg	$Cu\text{-}O_{eq}$	1.94 ± 0.01	4.96 ± 0.76	0.005 ± 0.001	−10.21
	$Cu\text{-}O_{ax}$	2.31 ± 0.02	1.24 ± 0.57	0.006[a]	
Dissolved humate	$Cu\text{-}O_{eq}$	1.94 ± 0.01	5.41 ± 0.85	0.005 ± 0.001	−6.95
	$Cu\text{-}O_{ax}$	2.32 ± 0.02	1.15 ± 0.63	0.006[a]	

[a] Constrained during fitting.

2.89 Å (Brown and Chidambaram, 1973). This Cu-C distance is greater than distances found in our study (2.24–2.32 Å).

For samples that contained between 0 and 88 g humic acid kg^{-1} goethite (Table 1), the peak between 2.7 and 3.2 Å in the RSFs (Fig. 6) corresponds to actual Cu-Fe distances between 3.17 and 3.20 Å. Higher-shell Fe(III) neighbors cannot be easily distinguished from Cu(II) because of similarities in their crystal ionic radii (Shannon, 1976) and number of electrons (hence backscattering amplitudes). However, a survey of Cu-Cu distances in different Cu oxide and hydroxide minerals revealed that shortest Cu-Cu distances typically range from 2.92 to 2.96 Å (Asbrink and Norrby, 1970; Ostwald et al., 1990). These compounds do contain additional Cu(II) atoms at greater distances; however, the coordination numbers determined with EXAFS were two to three times greater that those found in this study (Cheah et al., 2000). Because the intermetallic coordination numbers were less than those for CuO or $Cu(OH)_2$, we assumed that the higher shell metallic backscattering was attributable to Fe(III) atoms.

Figure 7 summarizes the data for Cu-O and Cu-Fe distances as a function of humic acid adsorbed on goethite. As shown in Figure 7 and in Table 1, the axial Cu-O distances decreased with increasing level of adsorbed humic acid between 0 and 28 g kg^{-1}, then increased for levels up to 88 g kg^{-1}. This trend in the axial Cu-O distances was consistent with observations on replicated sets of samples that were analyzed but not reported because the quality of the data was lower. With adsorbed humic acid $\leq$ 88 g kg^{-1}, the mean equatorial distances were between 1.96 and 1.97 ± 0.01Å for Cu(II) adsorbed on goethite and on goethite–humate complexes (Fig. 7; Table 1). For adsorbed humic acid concentrations $\geq$ 216 g kg^{-1} goethite, $Cu\text{-}O_{eq}$ distances were the same as for Cu(II) on humic acid (1.94 ± 0.01 Å), and higher-shell iron atoms were not identified because satisfactory fits were obtained without including higher-shell Fe(III) atoms in the fitting (see RSF fitting in Fig. 6).

4. DISCUSSION

4.1. Structure of Cu(II)-Surface Complexes

Analysis of the XANES and EXAFS data suggested that the Cu(II) coordination environment strongly resembles that of a type B ternary complex at adsorbed humate levels of 216 or 236 g kg^{-1}, where Cu(II) is bonded primarily to organic functional groups of the adsorbed humate. When Cu(II) is adsorbed to goethite–humate complexes containing humic acid at $\leq$88 g kg^{-1}, the metal appears to form an inner-sphere, bidentate complex with single iron octahedral sites (which contain two hydroxyls bonded to one iron). The trend of decreasing axial Cu-O bond length when adsorbed humic acid was between 0 and 28 g kg^{-1} also suggested that humic acid was bonded to Cu(II) that was simultaneously bonded to the goethite surface. At adsorbed humic acid levels from 14 to 28 g kg^{-1}, we propose that Cu(II) was primarily in type A ternary complexes (containing both organic and inorganic functional groups). These conclusions were based on the following detailed discussions of Cu-O and Cu-Fe coordination parameters.

4.2. Copper–Oxygen Coordination

EXAFS fitting results (Table 1) showed that for Cu(II) on goethite, the first coordination shell contains an average of 5.5 ± 0.9 oxygens at 1.96 ± 0.01 Å and ~1.6 ± 0.7 oxygens at 2.29 ± 0.03 Å. This type of arrangement indicates that Cu(II) ions are coordinated in distorted octahedra. In contrast, transition metals such as Ni(II), Co(II), and Cr(III) form holosymmetric complexes at mineral surfaces (Charlet and Manceau, 1992; O'Day et al., 1994; Scheidegger et al., 1997). The electronic configuration of Cu(II) causes it to undergo a Jahn-Teller distortion (Huheey, 1978) and adopt one of several distorted geometries that include square planar, square pyramidal, and tetragonal complexes (Asbrink and Norrby, 1970; Toman,

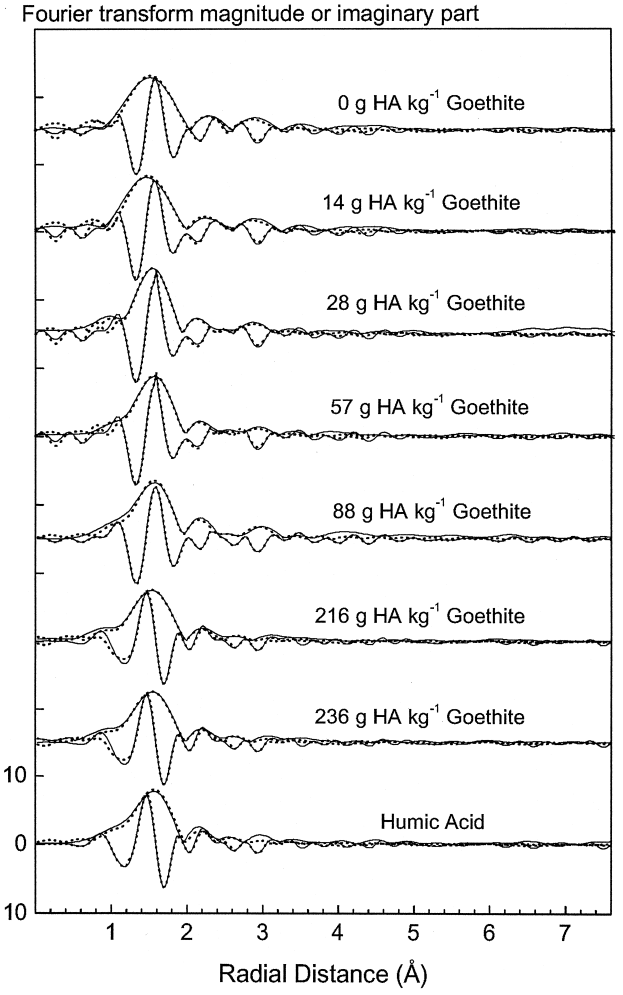

Fig. 6. Stacked radial structure functions showing the magnitude and imaginary parts of the Fourier-transformed EXAFS spectra for Cu(II) in aqueous solution, on goethite, on goethite with adsorbed humic acid, and on humic acid only. Solid and dotted lines represent the Fourier-transformed data and best fits, respectively. Radial distances are not corrected for phase shift.

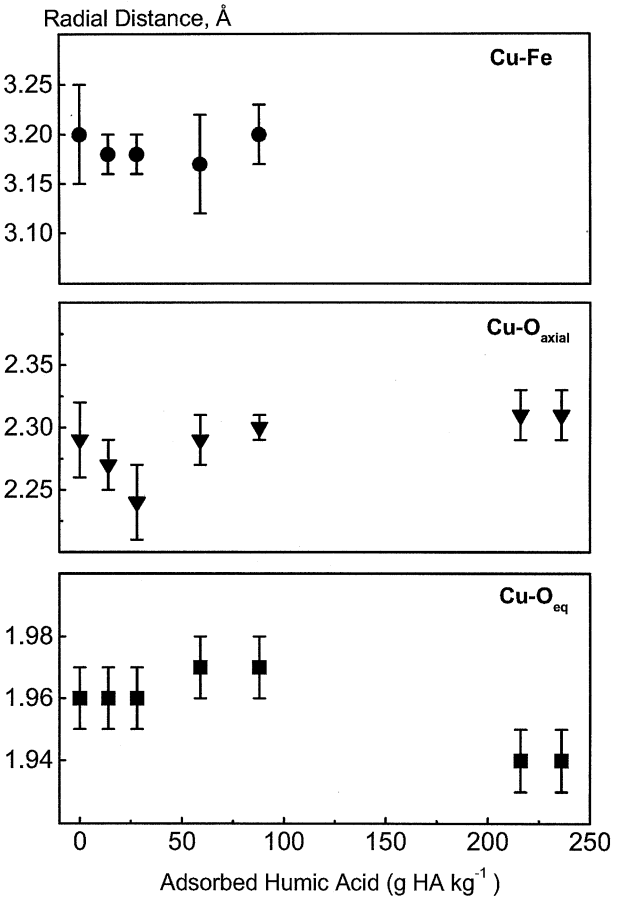

Fig. 7. Equatorial Cu-O (Cu-O_{eq}), axial Cu-O (Cu-O_{axial}), and Cu-Fe distances as a function of adsorbed humic acid concentration.

1977; Ostwald et al., 1990; Starova et al., 1991). The Jahn-Teller theorem states that the overall energy of a molecule can be lowered by decreasing the degeneracy and symmetry of the nonbonding and antibonding interactions (Huheey, 1978). For transition metals in an octahedral field (Fig. 8), d orbitals are arranged such that they contain double (e_g) and triple (t_{2g}) degeneracies (Huheey, 1978). For d^9 metals such as Cu(II), only three electrons occupy the higher-energy e_g level. The degeneracy of the e_g set of orbitals (d_{z^2} and $d_{x^2-y^2}$) is removed, thus stabilizing one of the two orbitals by lengthening either two axial or four equatorial metal ligand bonds. Stabilization of the occupied orbital ($2e^-$) at the expense of the partially filled orbital ($1e^-$) results in the observed distortions (Cotton and Wilkinson, 1988).

When the concentration of humate on the goethite surface was increased from 0 to 28 g kg^{-1}, a decrease in the mean Cu-O_{axial} distance (2.29–2.24 Å) was observed (Fig. 7; Table 1). Humic acids contain a diverse content of functional groups (Stevenson, 1994), each with unique abilities to polarize d orbitals in the coordinated metal ion and influence the ligand field splitting energy (LFSE). The LFSE is the energy difference between the e_g and t_{2g} sets of orbitals (Fig. 8; Huheey, 1978). The trend of decreasing Cu-O_{axial} distance for adsorbed humate between 0 and 28 g kg^{-1} is consistent with changes in the ligand field at the Cu(II) metal center. The relative ability of ligands to influence the LFSE has been measured and is referred to as the spectrochemical series (Huheey, 1978). The ligand field strength increases in the following order: $S^{2-} < OH^- < COOH < H_2O <$ pyridine $< NH_3$ (Huheey, 1978). Replacement of weaker-field equatorial ligands with stronger ligands increases the LFSE and the axial Cu–ligand distance. For example, it was observed that the Cu-O_{axial} distance increased from 2.27 to 2.44 Å when two or more pyridine or glycine ligands displaced water in the equatorial plane of Cu(II) ions (Ozutsumi and Kawashima, 1991; D'Angelo et al., 1998). When Cu(II) reacts with a humate–goethite complex, we propose that a ligand exchange reaction occurs in which water was replaced by weaker field carboxylic or phenolic ligands from the humic acid in an inner-sphere complex.

This can have opposite effects, depending on the order in which the Cu(II) is bonded in ternary complexes with goethite and humic acids. For type A complexes, the metal ion forms a bridge with the goethite surface and with the humic acid, and hence the LFSE decreases along with the Cu-O_{axial} distance

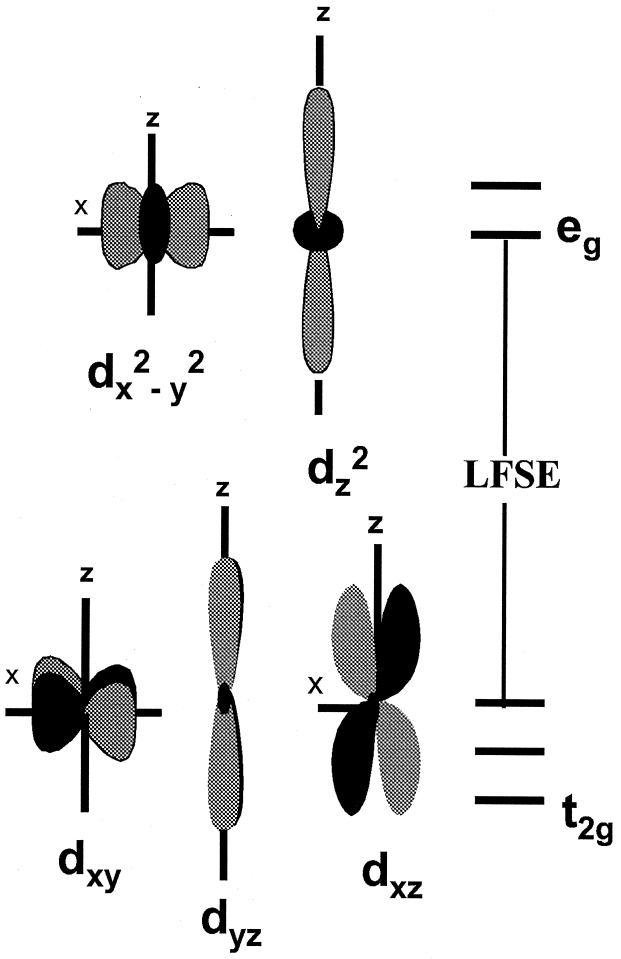

Fig. 8. Ligand field splitting energy (LFSE) and the arrangement of d orbitals in an octahedral field before distortion. Coordinating ligands approach the d orbitals along the x-, y-, and z-axes. A right-handed coordinate system is used for all of the orbitals.

because there are less water molecules bonded to Cu(II). In the case of type B complexes, the Cu(II) bonds strictly to adsorbed humic acid, and hence more water molecules (of greater ligand field strength) may coordinate to Cu(II) and increase the axial distance. Therefore, the decreasing trend in the axial Cu-O distance between 14 and 28 g humate kg^{-1} goethite suggests that the humic acid bonds with Cu(II) as a type A ternary complex. Type B complexes were dominant between 214 to 236 g humate kg^{-1} goethite, on the basis of the larger axial Cu-O distance. Samples with adsorbed humate levels of 59 and 88 g kg^{-1} may contain a combination of type A and type B ternary complexes.

Our proposed mechanism is consistent with that of previous studies involving Cu(II) with humic acids, in which a ligand exchange reaction was identified that involved the displacement of water molecules by carboxylic acid ligands (Bloom and McBride, 1979; Boyd et al., 1981a). The binding of Cu(II) by the humic acid occurred in equatorial positions (Boyd et al., 1981b). Hence, the decreasing Cu-O axial distances observed with goethite–humate complexes suggests that it is predominately weak field ligands such as carboxylic acids, rather than strong field amine or amide functional groups, that replace equatorial water molecules on Cu(II).

The XANES region is sensitive to changes in the ligand environment and can be used to provide an independent measure for estimating how electron transitions and multiple scattering are influenced by adsorbed humic acid. The decrease in the α peak intensity shows that the Cu(II) coordination environment depended on the concentration of adsorbed humic acid. Higher-shell iron atoms were identified for humic acid concentrations $\leq$ 88 g kg^{-1} goethite. If Cu(II) ions form a bridge (type A ternary complex) between the mineral surface and humic acid under these conditions, then a decrease in the α peak intensity is expected because stronger field water molecules undergo ligand exchanges with weak field organic groups (carboxylic or phenolic acids) in the equatorial plane of goethite-bound Cu(II) ions. The occurrence of a Type A ternary complex would explain the poorer XANES fits using only Cu(II) on goethite or on humic acid as end members, and the PCA results suggesting that a third species is needed to fit the derivative XANES spectra for Cu(II) on the goethite–humate complex.

At higher adsorbed humate levels, one would expect the proportion of Cu–humate bonding to increase if the adsorbed humic acid competes with Cu(II) for goethite surface sites. At concentrations between 218 and 236 g kg^{-1}, the α peak intensity (Fig. 3), the linear combination fitting (Fig. 4), and the $Cu\text{-}O_{eq}$ and $Cu\text{-}O_{axial}$ distances (Table 1) strongly indicated that Cu(II) bonded like that of Cu(II) with humic acid only. In addition, the inability to fit EXAFS spectra with higher-shell iron atoms at 218 and 236 g humate kg^{-1} further supports the argument most Cu(II) was not coordinated directly to goethite. Therefore, the XANES data support our conclusion that metal bonding reflects type B ternary complexes (goethite–humate–metal geometry) at adsorbed humic acid levels $\geq$ 218 g humic acid kg^{-1}.

In addition to multiple scattering effects, the XANES region also contains information about electron transitions. The main electron transition involves 1s electrons being excited to the continuum, which is largely populated by unfilled p states (Smith et al., 1985). Polarized EXAFS studies involving well-ordered single-crystal Cu(II) compounds have yielded significant experimental and theoretical information about $1s \rightarrow 4p_z$ electron transitions. It was found that the α peak intensity is influenced by the degree of axial distortion (Garcia et al., 1989) and by the covalency of the equatorial ligands bonded to the Cu(II) atom (Kau et al., 1987). The source of the α electron transition has been attributed to a shakedown effect, where the final electron state is lower in energy than the direct $1s \rightarrow 4p$ transition (Kau et al., 1987). The path to the final state involves a $1s \rightarrow 4p_z$ excitation combined with a ligand-to-metal charge transfer (Blair and Goddard, 1980).

As demonstrated by the 0.3 M $Cu(NO_3)_2$ spectra (Fig. 3), water molecules coordinated in the equatorial plane produce a strong α peak intensity. Humic acid molecules are much larger than water molecules. When comparing the derivative XANES spectra (Fig. 3) of Cu(II) in humic acid to 0.3 M $Cu(NO_3)_2$, the diminished α peak for the former suggests that the humic acid is more sterically hindered when approaching the Cu(II) and cannot bond in the equatorial plane with the same degree of angular overlap as water. Such steric hindrance would affect

the ability of the ligand to transfer charge to the metal when core electrons are removed in $1s \rightarrow 4p_z$ transitions.

4.3. Cu(II) Binding Sites on Goethite

Other EXAFS surface studies involving Cu(II) on goethite have shown the existence of Jahn-Teller distorted octahedra containing four short equatorial bonds and two elongated axial bonds (4 + 2) (Parkman et al., 1999). However, the average $Cu\text{-}O_{axial}$ distance obtained in our study (2.29 ± 0.03Å) was less than that determined by Parkman et al. (1999) (2.41 ± 0.02 Å). This discrepancy may be due to differences in the signal to noise ratios of the EXAFS data, which can strongly influence the ability to accurately determine coordination numbers and interatomic distances of distorted coordination shells (Heald, 1988).

In addition, sample preparation procedures could affect the axial Cu-O distance, particularly if precipitates formed at the mineral surface. In studies involving Cu(II) equilibrated with goethite suspensions at pH 8, $Cu(OH)_2(s)$ was the dominant phase (Bochatay et al., 1997; Parkman et al., 1999), as indicated by the resemblance in the intermetallic distances and coordination numbers. Approximately two Cu neighbors were identified at either 2.92 or 2.96 Å (Bochatay et al., 1997; Parkman et al., 1999). This result differs remarkably from the number of second metal neighbors (0.58 ± 0.39) found in our study at 3.20 ± 0.05 Å (Table 1). Therefore, we discounted the formation of Cu–hydroxy clusters or precipitates forming on the goethite surface because larger intermetallic coordination numbers were not observed, and because of differences in the reported distances.

The average Cu-Fe distance measured for the samples containing Cu(II) on goethite (3.20 ± 0.05 Å) gives insight into the surface configuration of adsorbed Cu(II). Most of the surface area of goethite is due to the 110 surface, with lesser amounts contributed by the 001, 100, and 010 surfaces (Schwertmann and Cornell, 1991; Barron and Torrent, 1996). Although the 110 surface is dominant, the surface chemistry of goethite is strongly influenced by hydroxyl groups that are singly coordinated with Fe on the 001 surface (Hiemstra et al., 1989). Hiemstra et al. (1989) modeled the reactivity of the 001 surface of goethite and found that $Fe\text{-}OH_2$ functional groups strongly contribute to the charging behavior of the mineral. Therefore, we suggest that Cu(II) reacted with the 001 surface and bonded with oxygens at single iron octahedral sites to form a bidentate edge-sharing complex.

If the geometry of the 001 surface is similar to that within the bulk goethite structure (i.e., no relaxation occurs), adsorption sites will contain O-Fe-O angles near 80°. The mineral howardevansite $[NaCuFe_2(VO_4)_3]$ was used as a model to evaluate Cu-Fe bond lengths for the proposed surface complex (Hughes et al., 1988). Howardevansite contains edge-shared Cu and Fe polyhedra with O-Fe-O angles of ~79°, which are similar to unrelaxed functional groups on the 001 goethite surface. The intermetallic Cu-Fe distance for howardevansite is 3.14 Å (Hughes et al., 1988), which compares favorably with the Cu-Fe distances found in our study (3.17–3.20 Å). This geometrical comparison suggests that edge-shared bidentate complexes ($^1E_{(001)}$) are plausible.

It is possible that Cu(II) also bonds to other surface sites on the goethite, given that the EXAFS spectrum reflects the average coordination environment. For example, hydroxyls that are single and doubly coordinated to iron are present on the 110 and 100 faces (Spadini et al., 1994) and could bind Cu(II) in such a way that only one iron atom is present. In addition, Cu(II) could bond on the 010 and 100 surface with oxygens that are coordinated with two iron neighbors. However, in all of these bonding configurations, Cu-Fe distances would range from 3.30 to 3.45 Å and thus are greater than our measured values of 3.17 to 3.20 Å for samples containing goethite. Again, our geometric calculations assume that the bond angles of the surface functional groups are similar to those in the bulk solid. A tridentate model involving face sharing between Cu(II) polyhedra and iron octahedra is not feasible because the Cu-Fe intermetallic distances would be less than 3.17 Å. An examination of the mineral hentschelite $[CuFe_2(PO_4)_2(OH)_2]$ best illustrates this point. With hentschelite, face sharing between Cu(II) polyhedra and iron octahedra produces intermetallic Cu-Fe distances of ~2.86 Å (Sieber et al., 1987). On the basis of these considerations, we conclude that the most probable bonding arrangement involves bidentate complexes that share edges with single iron sites at 001 faces (Fig. 9).

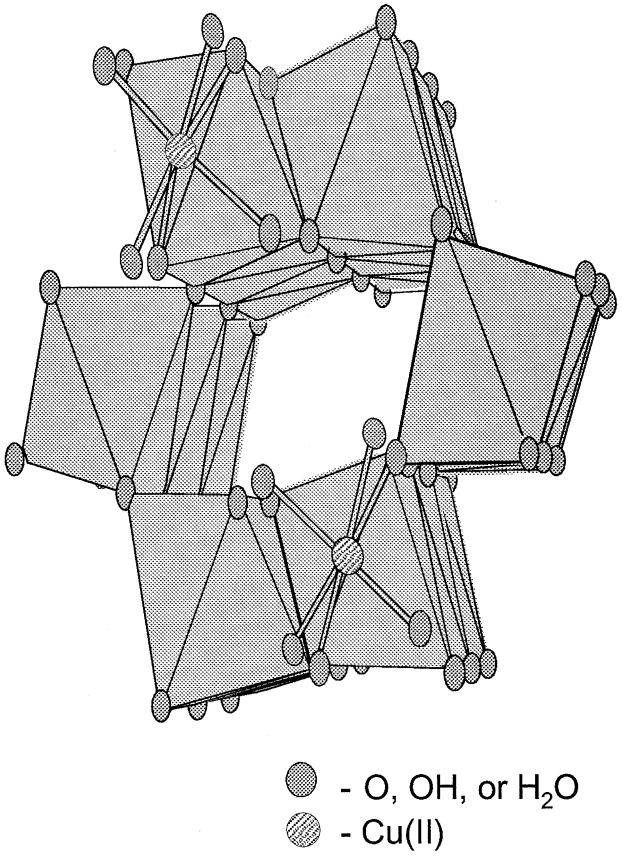

Fig. 9. Proposed coordination of Cu(II) in an edge-sharing, bidentate configuration with binding sites on the 001 surface of goethite.

5. CONCLUSIONS

Under the experimental conditions used here, analysis of XANES and EXAFS spectra indicated that Cu(II) was coordi-

nated predominantly with goethite–humate complexes as type A ternary complexes for adsorbed humic acid levels of 14 and 28 g kg^{-1} and type B ternary complex for levels between 216 and 236 g kg^{-1}. The type B ternary complex involves Cu(II) bound to humic acid, which in turn is bound to goethite. Unlike at lower adsorbed humate levels, humate levels with 216 and 236 g kg^{-1} showed no higher-shell Fe(III) atoms. The higher levels of adsorbed humic acid apparently made the goethite surface sites less accessible to Cu(II). The proposed type A complex involves Cu(II) bonded with goethite 001 surfaces as an inner-sphere complex, with humic acid involving carboxylic or phenolic acid functional groups. Our conclusions were based on EXAFS data showing average Cu-Fe distances of 3.17 to 3.20 Å for adsorbed humate levels $\leq$ 88 g kg^{-1}. With increasing adsorbed humic acid (0–28 g kg^{-1}), a decrease in axial Cu-O distance occurred, indicating that stronger-field water molecules were replaced with weak-field carboxylic or phenolic acid groups in the equatorial plane of surface-bound Cu(II) ions. Because clay–organic complexes are common in soils and sediments, ternary complexes involving Cu(II) are likely to occur and to influence the binding and dissolution of copper in these natural systems.

Acknowledgments—This research was funded by the National Science Foundation under grant EAR-9614920 and the North Carolina Agricultural Research Service. The authors are grateful to Ms. Kimberly Hutchinson for laboratory assistance. The research was carried out in part at the National Synchrotron Light Source, Brookhaven National Laboratory, Upton, NY, which is supported by the U.S. Department of Energy, Division of Materials Sciences, and Division of Chemical Sciences. Beamline X-11A was supported in part by U.S. Department of Energy contract DE-FG05-89ER45384.

Associate editor: D. L. Sparks

REFERENCES

Allison J., Brown D. S., and Nova-Gradac K. J. (1990) MINTEQA2/PRODEFA2, a geochemical assessment model for environmental systems [software]. Version 3.0. U.S. Environmental Protection Agency.

Asbrink S. and Norrby L. J. (1970) A refinement of the crystal structure of copper(II) oxide with a discussion of some exceptional E.s.d.'s. *Acta Cryst.* **B26,** 8–15.

Barron V. and Torrent J. (1996) Surface hydroxyl configuration of various crystal faces of hematite and goethite. *J. Colloid Interface Sci.* **177,** 407–410.

Bertsch P. and Seaman J. C. (1999) Characterization of complex mineral assemblages: Implications for contaminant transport and environmental remediation. *Proc. Natl. Acad. Sci. USA* **96,** 3550–3357.

Blair R. A. and Goddard W. A. (1980) Ab initio studies of x-ray absorption edges in copper complexes. 1. Atomic Cu^{2+} and $Cu(II)Cl_2$. *Phys. Rev. B* **22,** 2767–2776.

Bloom P. R. and McBride M. B. (1979) Metal ion binding and exchange with hydrogen ions in acid-washed peat. *Soil Sci. Soc. Am. J.* **43,** 687–692.

Bochatay I., Peterson P., Lovgren L., and Brown, G. E. Jr. (1997) XAFS study of Cu(II) at the water–goethite (α-FeOOH) interface. *J. Phys.* **IV C 2,** 819–820.

Bouldin C., Furenlid L., and Elam T. (1995) MACXAFS—An EXAFS analysis package for the Macintosh. *Physica B* **208/209,** 190–192.

Boyd S. A., Sommers L. E., Nelson D. W., and West D. X. (1981a) The mechanism of copper(II) binding by humic acid: An electron spin resonance study of a copper(II)–humic acid complex and some adducts with nitrogen donors. *Soil Sci. Soc. Am. J.* **45,** 745–748.

Boyd S. A., Sommers L. E., and Nelson D. W. (1981b) Copper(II) and iron(III) complexation by the carboxylate group of humic acid. *Soil Sci. Soc. Am. J.* **45,** 1241–1242.

Broome S. W. and Craft C. B. (2000) Tidal salt marsh restoration, creation, and mitigation. In *Reclamation of Drastically Disturbed Lands* (eds. R. I. Barnhisel, R. G. Darmody, and W. L. Daniels), pp. 939–959. American Society of Agronomy.

Brown G. M. and Chidambaram R. (1973) Dinuclear copper(II) acetate monohydrate: A redetermination of the structure by neutron-diffraction analysis. *Acta Cryst.* **B29,** 2393–2403.

Buffle J. (1988) *Complexation Reactions in Aquatic Systems: An Analytical Approach.* Halsted Press.

Charlet L. and Manceau A. (1992) X-ray absorption spectroscopic study of the sorption of Cr(III) at the oxide–water interface. *J. Colloid Interface Sci.* **148,** 443–458.

Cheah S. F., Brown G. E. Jr., and Parks G. A. (2000) XAFS study of Cu model compounds and Cu^{2+} sorption products on amorphous SiO_2, γ-Al_2O_3, and anatase. *Am. Mineral.* **85,** 118–132.

Cotton F. A. and Wilkinson G. (1988) *Advanced Inorganic Chemistry*. Wiley Interscience.

D'Angelo P. D., Boltari E., Festa M. R., Nolting H. F., and Pavel N. V. (1998) X-ray absorption study of copper(II)–glycinate complexes in aqueous solutions. *J. Phys. Chem. B* **102,** 3114–3122.

Davis J. A. (1984) Complexation of trace metals by adsorbed natural organic matter. *Geochim. Cosmochim. Acta* **48,** 679–691.

Douek M. and Ing J. (1989) Determination of sulfur and chlorine in pulp and paper samples by combustion/ion chromatography. *J. Pulp Paper Sci.* **15,** J72–J78.

Fitts J. P., Persson P., Brown G. E. Jr., and G. A. Parks. (1999) Structure and bonding of Cu(II)–glutamate complexes at the γ-Al_2O_3–water interface. *J. Colloid Interface Sci.* **220,** 133–147.

Frenkel A. I. and Korshin G. V. (1999) A study of non-uniformity of metal binding sites in humic substances by x-ray absorption spectroscopy. In *Understanding Humic Substances: Structures, Properties and Uses* (eds. E. A. Ghabbour and G. Davies), pp. 191–201. Royal Society of Chemistry.

Garcia J., Benfatto M., Natoli C. R., Bianconi A., Fontaine A., and Tolentino H. (1989) The quantitative Jahn-Teller distortion of the Cu^{2+} site in aqueous solution by XANES spectroscopy. *Chem. Phys.* **132,** 295–307.

Gee G. W. and Bauder J. W. (1986) In *Methods of Soil analysis. Part 1* (ed. A. Klute), pp. 383–411. American Society of Agronomy.

Heald S. (1988) Design of an EXAFS experiment. In *X-ray Absorption: Principles, Applications, Techniques of EXAFS, SEXAFS and XANES* (eds. D. C. Koningsberger and R. Prins), pp. 87–118. Wiley.

Hesterberg D, Sayers D. E., Zhou W., Robarge W. P., and Plummer G. M. (1997) XAFS characterization of copper in model aqueous systems of humic acid and illite. *J. Phys.* **IV C2,** 819–820.

Hiemstra T., De Wit J. C. M., and Van Riemsdijk W. H. (1989) Multisite proton adsorption modeling at the solid/solution interface of hydr(oxides): A new approach. *J. Colloid Interface Sci.* **133,** 105–117.

Hughes J. M., Drexler J. W., Campana C. F., and Malinconico M. L. (1988) Howardevansite, a new fumarolic sublimate from Izalco volcano, El Salvador: Description mineralogy and crystal structure. *Am. Mineral.* **73,** 181–186.

Huheey J. E. (1978) *Inorganic Chemistry: Principles of Structure and Reactivity*. Harper and Row.

Kau L. S., Spira-Soloman D. J., Penner-Hahn J. E., Hodgson K. O., and Solomon E. I. (1987) X-ray absorption edge determination of the oxidation state and coordination number of copper: Application to the Type 3 site in Rhus vernicifera Laccase and its reaction with oxygen. *J. Am. Chem. Soc.* **1987,** 6433–6442.

Kerndorff H. and Schnitzer M. (1980) Sorption of metals on humic acids. *Geochim. Cosmochim. Acta* **44,** 1701–1708.

Korshin G. V., Frenkel A. I., and Stern E. A. (1998) EXAFS study of the inner shell structure in copper(II) complexes with humic substances. *Environ. Sci. Technol.* **32,** 2699–2705.

Kunze G. W. and Dixon J. B. (1986) Pretreatment for mineralogical analysis. In *Methods of Soil Analysis, Part 1: Physical and Mineralogical Methods*,2nd ed. (ed. A. Klute), pp. 91–99. American Society of Agronomy.

Lindsay W. L. (1979) *Chemical Equilibria in Soils.* Wiley.

Lytle F. W., Sayers D. E., and Stern E. A. (1988) Report of the

international workshop on standards and criteria in x-ray absorption spectroscopy. *Physica B* **158,** 701–722.

Malinowski E. R. (1991) *Factor Analysis in Chemistry.* 2nd ed. Wiley.

McBride M. B. (1978) Transition metal bonding in humic acid: An ESR [electron spin resonance spectroscopy] study. *Soil Sci.* **126,** 200–209.

McBride M. B. (1994) *Environmental Chemistry of Soils*. Oxford University Press.

Nelson D. W. and Sommers L. E. (1996) Total carbon, organic carbon, and organic matter. In *Methods of Soil Analysis, Part 3: Chemical Methods* (ed. D. L. Sparks), pp. 961–1010. American Society of Agronomy.

Oades J. M. (1988) The retention of organic matter in soils. *Biogeochem.* **5,** 35–70.

O'Day P. A., Brown G. E. Jr., and Parks G. A. (1994) X-ray absorption spectroscopy of cobalt(II) multinuclear surface complexes and surface precipitates on kaolinite. *J. Colloid Interface Sci.* **165,** 269–289.

Ostwald H. R., Reller A., Schmalle H. W., and Dubler E. (1990) Structure of copper(II) hydroxide, $Cu(OH)_2$. *Acta Cryst.* **C46,** 2279–2284.

Ozutsumi K. and Kawashima T. (1991) EXAFS and spectrophotometric studies on the structure of pyridine complexes with copper(II) and copper(I) ions in aqueous solutions. *Polyhedron.* **11,** 169–175.

Palladino L., Della Longa S., Reale A., Belli M., Scafati A., Onori G., and A. Santucci. (1992) X-ray absorption near edge structure (XANES) of Cu(II)-ATP and related compounds in solution: Quantitative determination of the distortion of the Cu site. *J. Chem. Phys.* **98,** 2720–2726.

Parkman R. H., Charnock J. M., Bryon N. D., Livens F. R., and Vaughn D. J. (1999) Reactions of copper and cadmium ions in aqueous solution with goethite, lepidocrocite, mackinawite, and pyrite. *Am. Mineral.* **84,** 407–419.

Robertson A. P. and Leckie J. O. (1994) Humic acid/goethite interactions and their effect on copper binding. In *Humic Substances in the Environment and Implications on Human Health* (eds. N. Senesi and T. M. Miano), pp. 487–492. Elsevier Science.

Sayers D. E. and Bunker B. A. (1988) Data analysis. In *X-ray Absorption: Principles, Applications, Techniques of EXAFS, SEXAFS and XANES* (eds. D. C. Koningsberger and R. Prins), pp. 211–253. Wiley.

Scheidegger A. M., Lamble G. L., and Sparks D. L. (1997) Spectroscopic evidence for the formation of mixed-cation hydroxide phases upon metal sorption on clays and aluminum oxides. *J. Colloid Interface Sci.* **186,** 118–128.

Schellenberg K., Leuenberger C., and Schwartzenbach R. P. (1994) Sorption of chlorinated phenols by natural sediments and aquifer materials. *Environ. Sci. Technol.* **18,** 652–657.

Schwertmann U. and Cornell R. M. (1991) *Iron Oxides in the Laboratory.* VCH.

Senesi N. and G. Sposito. (1984) Residual copper(II) complexes in purified soil and sewage sludge fulvic acid: Electron spin resonance study. *Soil Sci. Soc. Am. J.* **48,** 1247–1253.

Shannon R. D. (1976) Revised effective ionic radii and systematic studies of interatomic distances in halides and chalcogenides. *Acta Cryst*. **A32,** 751–753.

Sieber N. H. W., Tillmanns E., and Hofmeister W. (1987) Structure of hentschelite, $CuFe_2(PO_4)_2(OH)_2$, a new member of the lazulite group. *Acta Cryst.* **C43,** 1855–1857.

Smith T. A., Penner-Hahn J. E., Berding M. A., Doniach S., and Hodgson K. O. (1985) Polarized X-ray absorption edge spectroscopy of single-crystal copper(II) complexes. *J. Am. Chem. Soc.* **10,** 5945–5955.

Spadini L., Manceau A., Schindler P. W., and Charlet L. (1994) Structure and stability of Cd^{2+} surface complexes on ferric oxides. *J. Colloid Interface Sci.* **168,** 73–86.

Sposito G. (1984) *The Surface Chemistry of Soils.* Oxford University Press.

Starova G. L., Filatov S. K., and Fundamensky L. P. (1991) The crystal structure fedotovite, $K_2Cu_3O(SO_4)_3$. *Mineral. Mag.* **55,** 613–616.

Stevenson F. J. (1994) *Humus Chemistry—Genesis, Composition, Reactions.* 2nd ed. Wiley.

Swift R. S. (1996) Organic matter characterization. In *Methods of Soil Analysis, Part 3: Chemical Methods* (ed. D. L. Sparks), pp. 1011–1069. American Society of Agronomy.

Tipping E., Griffith J. R., and Hilton J. (1983) The effect of adsorbed humic substances on the uptake of copper(II) by goethite. *Croat. Chem. Acta* **56,** 613–621.

Toman K. (1977) Symmetry and crystal structure of olivinite. *Acta Cryst.* **B33,** 2628–2631.

Vairavamurthy M. A., Maletic D., Wang S., Manowitz B., Eglinton T., and Lyons T. (1997) Characterization of sulfur-containing functional groups in sedimentary humic substances by x-ray absorption near-edge structure spectroscopy. *Energy Fuels* **11,** 546–553.

Xia K., Bleam W., and Helmke P. A. (1997) Studies of the nature of Cu^{2+} and Pb^{2+} binding site in soil humic substances using X-ray absorption spectroscopy. *Geochim. Cosmochim. Acta* **61,** 2211–2223.

Zabinski S. I., Rehr J. J., Ankudinov A., Albers R. C., and Eller M. J. (1994) Multiple-scattering calculations of x-ray absorption spectra. *Phys. Rev. B***52,** 2995–3009.